JMEPEG (2007) 16:549–553
DOI: 10.1007/s11665-007-9091-6

1059-9495/$19.00

Evaluation of Surface Residual Stresses in Friction Stir Welds Due to Laser and Shot Peening

Omar Hatamleh, Iris V. Rivero, and Jed Lyons

(Submitted August 23, 2006; in revised form September 5, 2006)

The effects of laser, and shot peening on the residual stresses in friction stir welds (FSW) has been investigated. The surface residual stresses were measured at five different locations across the weld in order to produce an adequate residual stress profile. The residual stresses before and after sectioning the coupon from the welded plate were also measured, and the effect of coupon size on the residual stress relaxation was determined and characterized. Measurements indicate that residual stresses were not uniform along the welded plate, and large variation in stress magnitude could be exhibited at various locations along the FSW plate. Sectioning resulted in significant residual stress relaxation in the longitudinal direction attributed to the large change in dimensions in this direction. Overall, laser and shot peening resulted in a significant reduction in tensile residual stresses at the surface of the specimens.

Keywords FSW, laser peening, residual stress, shot peening, x-ray diffraction

1. Introduction

Friction stir welding (FSW) is a relatively new welding technique invented by the Welding Institute in England in 1991 (Ref 1). FSW is a solid-state welding process that uses a nonconsumable cylindrical tool, i.e., rotated, plunged, and traversed along the weld joint. Conventional milling equipment and backside support are utilized to restrain the articles being welded. Material around the tool is frictionally heated, plasticized, and extruded to the back of the probe where it consolidates and cools.

In fusion welding, complex thermal and mechanical stresses develop in the weld and the surrounding areas. Following fusion welds, it is common for residual stresses to approach the yield strength of the base material. FSW takes place at a low-temperature level compared to fusion welding; therefore, residual stresses may be considerably less than those in fusion welds. However, the heating cycle of the material experiences during welding, and the rigid clamping arrangement used in FSW can have an impact on residual stresses in the weld. For example the rigid clamping arrangement used in FSW imposes higher restraints on the welded plates than the more compliant clamps used for fixing the parts during conventional welding processes. The restraints imposed by the FSW clamps prevent the contraction of the weld nugget and heat affected zone in the longitudinal and transverse direction due to cooling (Ref 2, 3). This in return will introduce transverse/longitudinal residual stresses in the weld.

The residual stresses developed during the welding process can have a significant effect on the service performance of the welded material with respect to fatigue properties, and fatigue crack growth process. Residual tension stresses in the weld can lead to faster crack initiation and propagation, and could also result in stress corrosion cracking (SCC). Surface processing technique like laser and shot peening can help to relieve a significant amount of these residual stresses.

The use of FSW is expanding and is resulting in welded joints being used in critical load bearing structures. Therefore the investigation of the residual stress distribution in FSW is important and needs to be well-understood.

Laser peening (LP) is a technique with the capability to introduce a state of residual compressive stresses that can significantly increase fatigue properties (Ref 4, 5). Previous research (Ref 6, 7) has shown that the residual stress resulting from laser peening can be significantly higher and deeper than for conventional shot peening.

In this investigation the effects of laser, and shot peening on the residual stresses in FSW will be investigated. The surface residual stresses will be measured at five different locations across the weld in order to produce an adequate residual stress profile. To establish a baseline, measurements will also be taken on a coupon without any peening. The residual stresses before and after sectioning a coupon from the welded plate will also be measured, and the effect of coupon size on the residual stress relaxation will be determined and characterized.

2. Experimental Procedures

The laser peening process (shown in Fig. 1) utilizes high-energy laser pulses (several GW/cm^2) fired at the surface of a metal coated with an ablative film, and covered with a transparent layer (usually water). As the laser beam passes

Omar Hatamleh, Structures & Dynamics Branch, NASA-Johnson Space Center, Houston, TX 77058; **Iris V. Rivero,** Industrial Engineering Department, Texas Tech University, Lubbock, TX 79409-3061; **Jed Lyons,** Mechanical Engineering Department, University of South Carolina, Columbia, SC 29208. Contact e-mail: omar.hatamleh-1@nasa.gov.

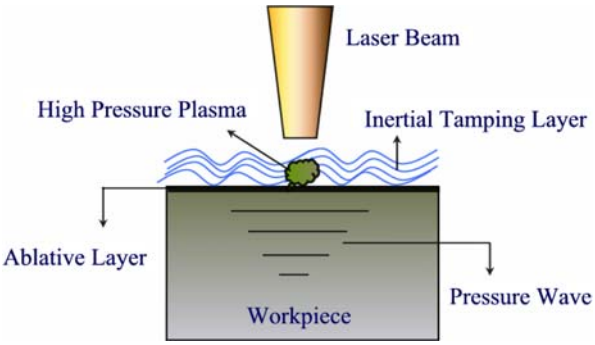

Fig. 1 Laser peening process

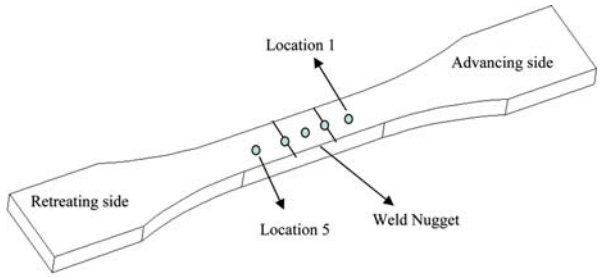

Fig. 2 Residual stress measurements points

through the transparent layer and hits the surface of the material, a thin layer of the ablative layer is vaporized. The vapor continues to absorb the remaining laser energy and is heated and ionized into plasma. The rapidly expanding plasma is trapped between the sample and the transparent layer, creating a high-surface pressure, which propagates into the material as a shock wave (Ref 8).

When the peak pressure of the shock wave is greater than the dynamic yield strength of the material, it produces plastic deformation in the metal. The actual depths of the LP-induced stresses will vary depending on the type of material, and the laser peening processing conditions chosen (Ref 9). Laser peening has also been reported to increase the dislocation density in aluminum alloys, but no quantitative analysis has been noted (Ref 6).

The laser peening for this investigation was performed at the Metal Improvement Company in Livermore California. The surface of the specimens intended for peening was covered with an aluminum tape 0.22 mm thick, and was replaced in between layers of peening. The tamping layer consisted of an approximately 1 mm thick laminar layer of flowing water. The laser peening was applied using a square laser spot size of 4.72 × 4.72 mm^2 with a laser power density of 2 GW/cm^2 and 18 ns in duration. The laser-peened specimen used for the residual stress investigation was peened with three layers of laser peening, and the spots within a layer were overlapped 3%. Peening between layers had an offset of 33% in the two in plane directions. A peening frequency of 2.7 Hz and a 1 micron wavelength laser was employed. Both sides of the specimen were shocked using the same conditions. The shot peened specimen was accomplished using 0.059 mm glass beads with an Almen intensity of 0.008-0.012A and a 200% coverage rate.

The surface residual stresses for the FSW specimens were measured through x-ray diffraction (XRD). Particularly, residual stresses were determined by the Multiple Exposure Technique (MET). When measuring residual stresses through XRD, the strain in the crystal lattice is measured, and the residual stresses inducing the strain are calculated. When calculating residual stresses it is assumed that the crystal lattice is linearly distorted. The premise of the MET is that the atomic spacing (d) between crystallographic planes that are equal "will vary consistently with their psi (ψ) angle" (Ref 10) where the ψ angle is defined as the "angle between the surface normal and the normal to the crystallographic planes from which the x-ray peak is diffracted" (Ref 10). Therefore, to determine the magnitude of residual stresses lattice strains are assessed in various ψ directions and a plot of $\sin^2\psi$ vs. $\varepsilon_{\phi\psi}$ is derived (where ϕ is the angle between a reference direction and the direction of stress measurement in the plane). $\varepsilon_{\phi\psi}$ is the strain in the ϕ and ψ directions defined by Hilley et al. (Ref 11):

$$\varepsilon_{\phi\psi} = \frac{1+\nu}{E}\left(\sigma_\phi \sin^2\psi\right) - \frac{\nu}{E}(\sigma_1 + \sigma_2) \qquad \text{(Eq 1)}$$

where ν = Poisson's ratio, σ_ϕ = surface stress at an ϕ angle with a principal stress direction, E = modulus of elasticity, σ_1, σ_2 principal stresses.

Then from the $\sin^2\psi$ vs. $\varepsilon_{\phi\psi}$ plot, residual stresses are established through the following relation (Ref 11):

$$\sigma_\phi = \frac{mE}{1+\nu} \qquad \text{(Eq 2)}$$

where m = slope of the $\sin^2\psi$ vs. $\varepsilon_{\phi\psi}$ plot.

While performing the MET in this research study a Cr target x-ray tube was used and energized at 25 kV and 7 ma. The Bragg angle selected for diffraction was 162° capturing diffraction from the 333 and 511 planes. Ten exposures were collected per location for 5 s of duration per exposure with maximum β angle of 24° and 10β angle tilts. Residual stresses were measured in both the transverse and the longitudinal directions at five locations across the weld as illustrated in Fig. 2. The locations corresponded to the weld centerline, weld interface, and the HAZ.

3. Results and Discussion

3.1 Residual Stress along the Welded Plate

To assess the residual stresses variation along the welded plate, residual stress measurements were made at 12, 22, and 32 cm from the start of the FSW at "location 4" as indicated in Fig. 2. The measured residual stresses at the different locations along the weld were 91, 92.4, and 59.9 MPa in the longitudinal direction, and 19.3, −4.8, and 5.5 MPa in the transverse direction, respectively. These measurements indicate that residual stresses were not uniform along the welded plate, even when measured at the same distance from the weld centerline. This could be possible due to the clamping configuration used in the welding process, or could also be attributed to the changes in the heat cycle experienced during welding. Because of this variation in residual stresses, fatigue scatter for FSW specimens cut from different locations along the plate may be higher than specimens produced from base material.

3.2 Residual Stress Relaxation

To evaluate the residual stresses as a function of coupon size, two coupons sizes with two different widths 1.27 and 1.9 cm were used as shown in Fig. 3. A single point at the tool shoulder boundary on the retreating side (location 4 in Fig. 2) was chosen to measure the stresses. The stresses in both the longitudinal and transverse direction were measured using the x-ray diffraction method. To quantify the residual stress relaxation, specimens were cut from the FSW plate using a wire EDM, and stresses were re-measured again at the same location. The residual stresses are summarized in Table 1.

In all cases the stresses in the (width) longitudinal direction exhibited significant relaxation and became more compressive after sectioning. These results indicate that the elastic strains changed due to the sectioning process, and residual stresses were altered by the large reduction in the width. Measurements in the (length) transverse direction changed only slightly. The small coupon did not show a statistically significant change while the large coupon showed a slight tensile increase.

These results indicate that sectioning did cause significant residual stress changes in the samples in the longitudinal direction attributed to the large change in dimensions in this direction. Changes in the transverse direction were not as large because the coupon lengths were large relative to the plate size. It should be noted that all these measurements were taken at the surface; subsurface measurements may exhibit different values. Measurement taken at other locations at the surface are also expected to increase or decrease depending on the location relative to the weld centerline and direction of the residual stresses being measured.

The surface residual stresses for different samples with different widths were quantified at different locations across the weld. The measurements were collected using the XRD in both longitudinal and transverse directions. The dimensions of the specimens and residual stress measurement locations are illustrated in Fig. 4.

A summary of the surface residual stress measurements per location is provided in Table 2-4 below. An accurate assessment of the residual stress relaxation is unavailable without comprehensive residual stress measurements on the as welded

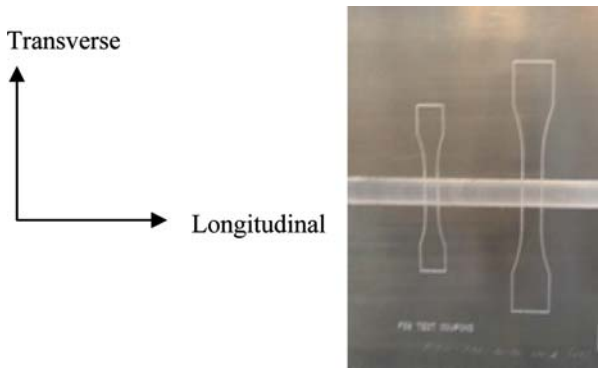

Fig. 3 FSW coupons used for residual stress measurements

Table 1 Residual stress summary

		Residual stress, MPa	
Sample	**Direction**	**Before sectioning**	**After sectioning**
Small coupon	Longitudinal	91 ± 12.4	−11 ± 11.7
	Transverse	19.3 ± 8.3	6.9 ± 8.3
Large coupon	Longitudinal	92.3 ± 13.8	19.3 ± 15.2
	Transverse	−4.8 ± 8.96	28.2 ± 8.2

Table 2 Stress measurements for the 10.16 cm wide coupon

Location	Longitudinal residual stress, MPa	Transverse residual stress, MPa
1	−75.77 ± 143.27	179.33 ± 95.15
2	140.72 ± 86.94	−32.26 ± 40.12
3	12.34 ± 4.12	−14.20 ± 2.76
4	75.70 ± 37.37	−90.32 ± 49.16
5	477.48 ± 204.71	−164.58 ± 135.21

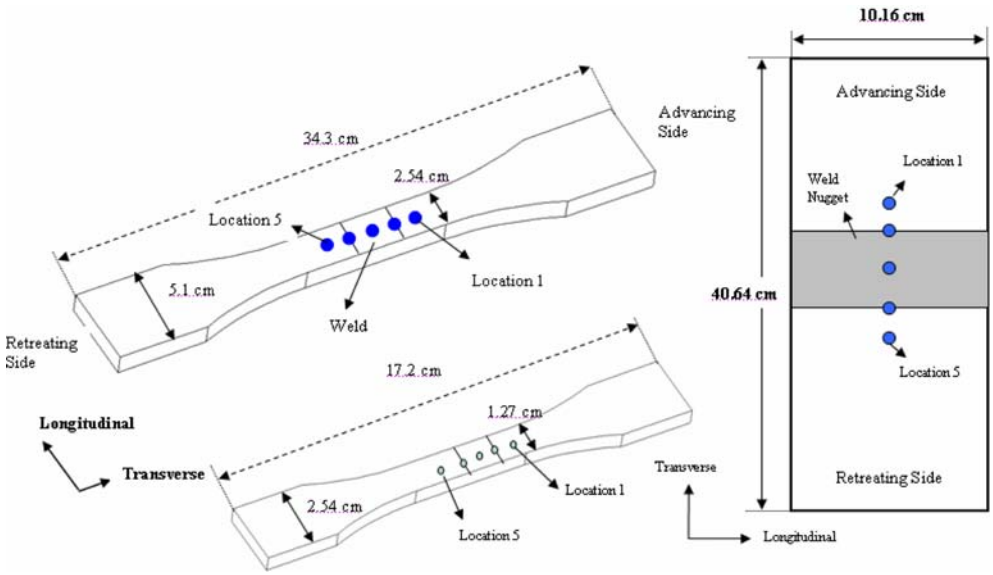

Fig. 4 Geometry for specimens used for residual stress measurements

plate before the specimen were cut. Nevertheless, the results indicate that a significant amount of residual stresses can still be present after sectioning the samples from the welded plate. These residual stresses can still have significant effects on the fatigue initiation and propagation through changes to the effective mean stress during the fatigue cycling.

X-ray equipment alignment, extreme preferred orientation, excessive surface roughness or curvature, and precise knowledge of the proper elastic constant to convert the x-ray measured strain into stress can cause the overall accuracy to decrease. However, the larger scatter in the residual stress measurements from x-ray diffraction usually arises from measuring materials with large grain size. Relatively large grains in the base material can significantly affect the accuracy of the measured residual stresses. Conversely, the fully recrystallized fine-grain microstructure in the weld nugget will provide a larger sampling of grains; therefore, improving the accuracy of the x-ray diffraction measurements as evident in the measurements taken at location 3 in the previous tables. Measurement scatter in the HAZ will reflect the larger grain microstructure, and the scatter in the measurements due to the large grain structure will preclude accurate residual stress measurements. Large scatter in x-ray diffraction measurements in the HAZ due to larger grain size was also reported by James (Ref 12) on 7050 AA. It is possible that using a larger size collimator may have resulted in more accurate results, since higher number of grains may be sampled.

Table 3 Stress measurements for the 2.54 cm wide coupon

Location	Longitudinal residual stress, MPa	Transverse residual stress, MPa
1	−15.85 ± 161.85	−14.54 ± 98.39
2	18.54 ± 9.87	−37.78 ± 26.89
3	3.58 ± 3.17	−33.64 ± 2.55
4	−76.98 ± 102.04	119.97 ± 88.04
5	19.98 ± 229.56	361.29 ± 168.03

Table 4 Stress measurements for the 1.27 cm wide coupon

Location	Longitudinal residual stress, MPa	Transverse residual stress, MPa
1	−48.67 ± 120.38	−221.46 ± 66.95
2	−18.82 ± 10.68	−58.34 ± 36.26
3	−16.13 ± 4.41	−12.82 ± 2.20
4	73.56 ± 54.53	−13.16 ± 40.12
5	146.51 ± 114.52	26.61 ± 97.90

3.3 Surface Residual Stress for the Laser and Shot Peened Specimens

To quantify the effects from the laser peening and shot peening on the surface residual stress, stresses were measured on the FSW peened and unpeened specimens using the x-ray diffraction technique. The measurements were taken in both the longitudinal and transverse directions at five different locations as indicated in Fig. 2. The residual stresses at different locations across the weld are shown in Fig. 5 and 6. It can be seen from Fig. 5 and 6 that laser and shot peening resulted in a significant reduction in tensile residual stresses at the surface of the specimens. These compressive stresses can have a significant impact on the fatigue life of the specimens.

In Fig. 5, the residual stress measurement in the advancing side of the weld (location # 1 in Fig. 2) for the laser-peened specimen shows a significant compressive stress value (−663.29 MPa). The physical significance of this measurement is questionable, since this value is significantly higher than the yield stress of the material. However, the measurement suggests that high-compressive residual stresses are present at that location.

4. Summary and Conclusions

The residual stresses at different distances from the FSW starting point were measured to assess the variation in residual stresses along the welded plate. Measurements indicate that residual stresses were not uniform along the welded plate, and large variation in stress magnitude could be exhibited at various locations along the FSW plate. The residual stresses before and after sectioning the coupon from the welded plate were also measured. These results indicate that sectioning did cause significant changes in stresses in the width (longitudinal) direction attributed to the large change in dimensions in this direction. Changes in the length (transverse) direction were not

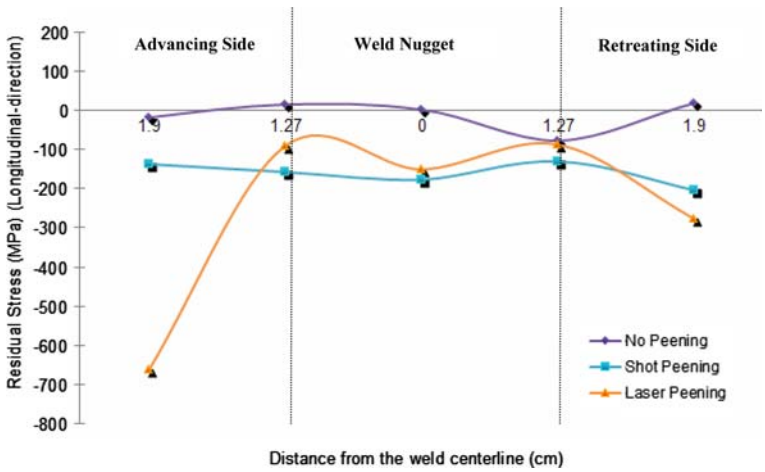

Fig. 5 Residual stress distributions across the weld (Longitudinal direction)

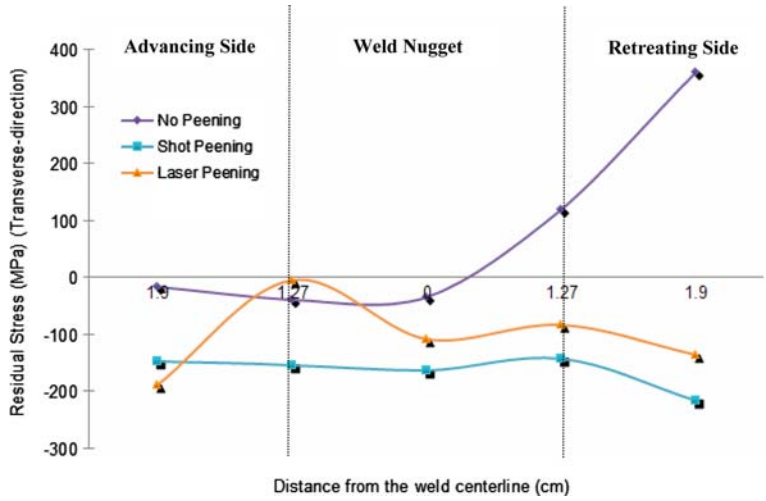

Fig. 6 Residual stress distributions across the weld (Transverse direction)

as large because the coupon lengths were large relative to the plate size.

To quantify the effects of laser and shot peening on the surface residual stresses, the surface residual stresses for the FSW peened specimens were measured at five different locations across the weld, and were then compared to an unpeened FSW specimen. Laser and shot peening resulted in a significant reduction in tensile residual stresses at the surface of the specimens. Although the residual stress profile for the shot peening was fairly uniform across the weld with an average value of 158.97 MPa in the longitudinal direction, and 163.86 MPa in the transverse direction. Laser peening on the other hand exhibited more variation at different locations across the weld. For example a compressive residual stress around −663.29 MPa was measured in the longitudinal direction at "Location 1" (Fig. 2) which corresponds to 7.5 mm from the weld interface, and a −86.7 MPa at "Location 4." Conversely a transverse compressive residual stress around −188.37 MPa was measured at "Location 1," and −3.30 MPa at "Location 2." The highest tensile residual stress in the unpeened specimen was around 477.48 MPa in the longitudinal direction for the 10.16 cm wide specimen, while a maximum tensile residual stress of 361.29 MPa was measured in the transverse direction for the 2.54 cm wide specimen. A large scatter in the residual stress measurements from the x-ray diffraction was identified in the HAZ and was attributed to the large grain size in that region of the weld.

References

1. W.M. Thomas, E.D. Nicholas, J.C. Needham, M.G. Murch, P. Temple-Smith, and C.J. Dawes, Friction Stir Butt Welding, Int Patent App PCT/GB92/02203, and GB Patent App 9125978.8, December 1991, US patent No. 5, 460,317, October 1995
2. R.S. Mishra and Z.Y. Ma, Friction Stir Welding and Processing, *Materials Science and Engineering*, 2005, **R50**, p 1–78
3. C. Dale Donne, E. Lima, J. Wegener, A. Pyzalla, and T. Buslaps, Investigations on Residual Stresses in Friction Stir Welds, *3'rd International Symposium on Friction Stir Welding*, Kobe, Japan, 2001
4. J.M. Yang, Y.C. Her, N. Han, and A. Clauer, Laser Shock Peening on Fatigue Behavior of 2024-T3 Al Alloy with Fastener Holes and Stopholes, *Materials Science and Engineering*, 2001, **A298**, p 296–299
5. C. Rubio-Gonzalez, J.L. Ocana, G. Gomez-Rosas, C. Molpeceres, M. Paredes, A. Banderas, J. Porro, and M. Morales, Effect of Laser Shock Processing on Fatigue Crack Growth and Fracture Toughness of 6061-T6 Aluminum Alloy, *Materials Science and Engineering*, 2004, **A386**, p 291–295
6. C. Montross, T. Wei, L. Ye, G. Clark, and Y. Mai, Laser Shock Processing and its Effects on Microstructure and Properties of Metal Alloys: A Review, *International Journal of Fatigue*, 2002, **24**, p 1021–1036
7. P. Peyre, R. Fabbro, P. Merrien, and H.P. Lieurade, Laser Shock Processing of Aluminium Alloys. Application to High Cycle Fatigue Behaviour, *Material Science and Engineering*, 1996, **A210**, p 102–113
8. Y. Tan, G. Wu, J. Yang, and T. Pan, Laser Shock Peening on Fatigue Crack Growth Behavior of Aluminum Alloy, *Fatigue and Fracture of Engineering Materials*, 2004, **27**, 649–656
9. J.K. Gregory, and H.J. Rack, and D. Eylon eds., *Surface Performance of Titanium*. TMS, Warrendale, PA, 1996, 217–230
10. C.O. Ruud and D.F. Carpenter, *Operators Manual for the D-1000-A Stress Analyzer*. Denver X-Ray Instruments, Incorporated, Englewood, 1985
11. M.E. Hilley, Ed., J.A. Larson, Assoc. Ed., C.F. Jatczak, Assoc. Ed., and R.E. Ricklefs, Assist. Ed., *Residual Stress Measurement by X-ray Diffraction SAE J784a*, Society of Automotive Engineers, Inc., New York, 1971
12. M. James, M. Mahoney, and D. Waldron, Residual Stress Measurements in Friction Stir Welded Aluminum Alloys, *Proceedings of the First International Symposium on Friction Stir Welding*, USA, June 14-16, 1999